

Cross-sections and experimental signatures for detection of a well-defined dark matter WIMP

BAILEY TALLMAN¹, JEHU MARTINEZ¹, ROHAN SHANKAR¹, KANE RYLANDER¹ and ROLAND E. ALLEN¹

¹ *Physics and Astronomy Department, Texas A&M University, College Station, Texas 77843, USA*

Abstract – We report the following calculations for a recently proposed bosonic dark matter WIMP with well-defined interactions: (1) the mass as determined by fitting to the relic abundance; (2) the current annihilation cross-section for indirect detection; (3) cross-sections for pair production accompanied by jets in proton colliders with center-of-mass energies ranging from 13 to 100 TeV; (4) for the high-luminosity LHC, and planned 100 TeV proton collider, detailed plots of experimentally accessible quantities before and after optimal cuts; (5) cross-sections, and plots of experimentally accessible quantities, for production in e^+e^- or muon colliders with center-of-mass energies up to 10 TeV; (6) cross-section per nucleon for direct detection. The conclusions are given in the text, including the principal prediction that (with optimal cuts) this particle should be detectable at the high-luminosity LHC, perhaps after only two years with an integrated luminosity of 500 fb⁻¹.

Introduction. – In a previous letter [1], and subsequent papers [2–4], we proposed a bosonic dark matter WIMP with precisely-defined interactions which are weak and second-order, implying low cross-sections that are consistent with experiment. Here we report much more extensive calculations relevant to its experimental detection within the near and more distant future [5–10].

All these calculations were performed with the interactions in Eq. (47) of [1], using MicrOMEGAs [11], MadGraph [12], and MadAnalysis [13].

Annihilation cross-section and mass from relic density. – Fig. 1 shows our results (obtained with MicrOMEGAs) for the variation of the standard parameter $\Omega_{DM}h^2$ with the mass of the present dark matter particle, which is designated h^0 and called a higgson as in our previous papers, because of its close relationship to the observed Higgs boson H^0 .

Here $\Omega_{DM} = \rho_{DM}/\rho_c$, where ρ_{DM} is the current density of dark matter and ρ_c is the critical density. Also, $h = H_0/(100 \text{ km s}^{-1}\text{Mpc}^{-1})$, where H_0 is the current value of the Hubble parameter.

If the present particle accounts for all or the great majority of the dark matter, it can be seen that its mass is close to 70 GeV for all values of h within the range of currently accepted values [14].

Even in a multicomponent scenario where it is a substantial component, it still must have a mass below the 80

GeV mass of the W boson, since otherwise it would undergo rapid annihilation in the early universe. This means that the results below for collider detection still hold approximately for all scenarios in which the present particle constitutes a significant fraction of the dark matter.

The cross-section for annihilation in the present universe is shown as a function of mass in Fig. 2. For a mass of 70 GeV, our calculations yield a cross-section given by $\langle\sigma_{ann}v\rangle = 1.19 \times 10^{-26} \text{ cm}^3/\text{s}$. This value is consistent with the current limits from observations of dwarf galaxies [10, 15–17] (for a particle mass of 70 GeV and annihilation into e.g. W^+W^- pairs). Our calculated mass and $\langle\sigma_{ann}v\rangle$ are also both consistent with analyses of the Galactic center gamma-ray excess observed by Fermi-LAT [18–23] and the antiproton excess observed by AMS-02 [24–28], as well as the multitude of observations by other experiments [10, 29, 30], although only the gamma-ray excess is currently regarded as potentially strong evidence of dark matter annihilation.

At one time it may have appeared that a positron excess from AMS-02 and other experiments was evidence for a dominant dark matter particle at an energy of ~ 800 GeV or above. However, this interpretation has been ruled out by Planck [30], and the excess has been attributed to pulsars [31].

Among many other astrophysical implications, the present dark matter candidate is consistent with the formation of “dark stars” in the early universe [32].

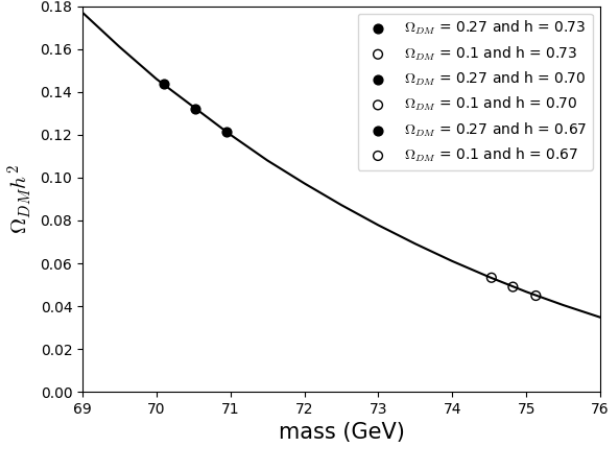


Fig. 1: $\Omega_{DM}h^2$ versus mass of the present dark matter WIMP. For the three points on the left, with a dark matter fraction of 27% and three possible values of the Hubble parameter h [14], the higgson is assumed to comprise most of the dark matter. The mass is then near 70 GeV in each case. For the points on the right the higgson is taken to be subdominant in a multicomponent scenario, contributing only a 10% fraction of the observed mass-energy content of the universe. The mass is then still not far from 70 GeV, and this is true even for substantially smaller fractions. The reason is that this particle would be extremely subdominant if the mass were above 80 GeV, permitting rapid annihilation into W bosons.

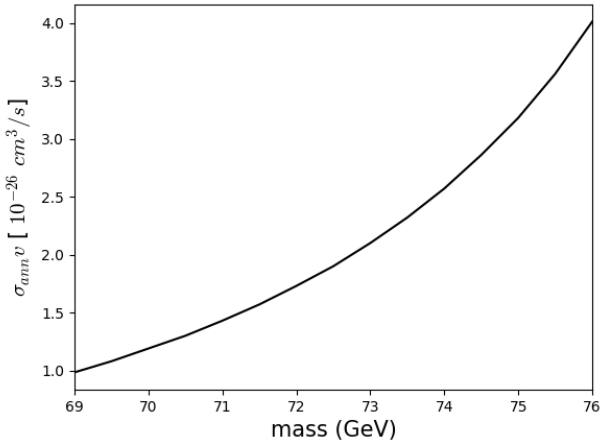


Fig. 2: $\langle\sigma_{ann}v\rangle$ versus mass for the present dark matter WIMP. For the mass of 70 GeV established by the calculations shown in Fig. 1, $\langle\sigma_{ann}v\rangle = 1.19 \times 10^{-26} \text{ cm}^3/\text{s}$. Larger masses would imply a smaller relic abundance, still consistent with the observational limits.

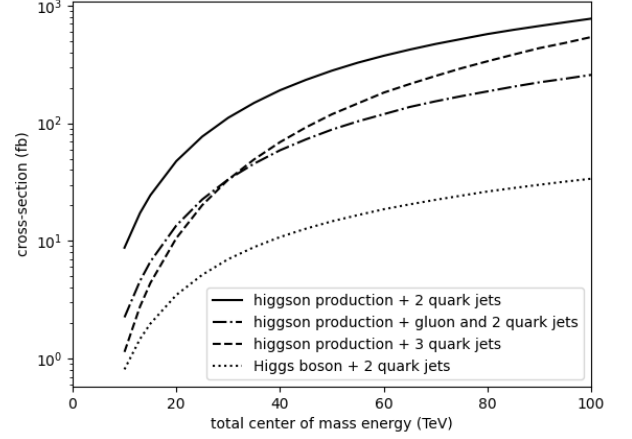


Fig. 3: Cross-sections for production of the present particle – called a higgson in our previous papers – in proton colliders with center-of-mass energies \sqrt{s} up to 100 TeV. For the 14 TeV high-luminosity LHC the cross-section is 20 fb. The similarly calculated cross-section for production of a Higgs boson pair through vector boson fusion is also shown.

Production cross-sections and experimental signatures in proton colliders. – Using MadGraph and MadAnalysis, we have calculated cross-sections for production of the present dark matter particle h^0 in proton colliders with center-of-mass energies from 13-14 TeV (for the current and high-luminosity LHC) to 100 TeV (for the ultimate performance of the proposed future circular collider [33]). The results for various signals are shown in Fig. 3.

Fig. 3 also shows our results for vector-boson-fusion (VBF) production of Higgs boson pairs, which are generally consistent with those of previous calculations [34–45] (where it was found that the cross-section was sufficiently large for VBF to be a promising route to observing and measuring the HHH and $HHVV$ interactions, with H and V respectively representing the Higgs and vector boson fields).

We now give two examples of how the present particle can be discovered in proton colliders, with a small fraction of the results for observables shown in Figs. 4-9.

First example – higgson pair accompanied by 2 quark jets, with 14 TeV center of mass energy and 500 fb^{-1} integrated luminosity. In Fig. 3 it can be seen that the largest cross-section is for production of a higgson pair accompanied by a pair of quark jets. We therefore focus on this process in searching for optimized cuts at 14 TeV center of mass energy. The standard model background for this single process is a neutrino pair accompanied by two quark jets.

Below, j_1 and j_2 are the two quark jets, p_T is the transverse momentum, η is the pseudorapidity, and other quan-

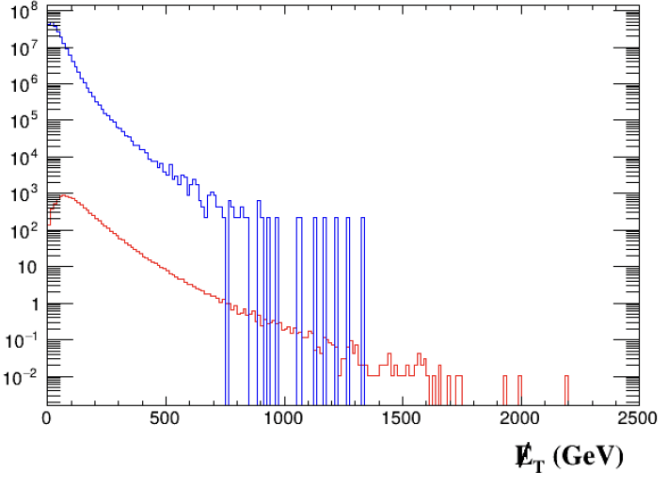


Fig. 4: Anticipated number of events as a function of the “missing transverse energy” E_T (as defined in [12] and [13]), for an integrated LHC luminosity of 500 fb^{-1} and center-of-mass energy $\sqrt{s} = 14 \text{ TeV}$, prior to any cuts on the observables. (For all the histograms of this paper, 200 bins were used.) Here and in Figs. 5-7, the higher histograms are those for background. The calculations were done with 10^6 events for the specified signal – a pair of higgsos accompanied by 2 quark jets – and 10^6 events for the standard model background – a pair of neutrinos accompanied by 2 quark jets. The fluctuations in histogram height, here and in the plots below, are much larger for the background because the number of events was taken to be the same for signal and background in the calculations, but the total calculated cross-section is 20.6 fb for the signal and 436 pb for the background, so that the total anticipated number of events is about 21000 times larger for background, making the height for a single calculated event 21000 times larger.

tities are defined in [12] and [13]. The final optimized cuts (obtained after many one-million-event runs) are the following:

Cut 1: p_T of $j_2 < 250 \text{ GeV}$

Cut 2: $|\eta_{j_1} - \eta_{j_2}| > 3$

Cut 3: $|\eta_s| > 1.5$ for “vector sum” of quark jet momenta

Cut 4: energy of $j_1 > 420 \text{ GeV}$

Cut 5: energy of $j_2 > 420 \text{ GeV}$

Cut 6: $|\eta_d| > 3.15$ for “vector difference” of jet momenta

Cut 7: sum of quark jet energies $> 1500 \text{ GeV}$

Cut 8: “missing transverse energy” $> 70 \text{ GeV}$

Cut 9: “invariant mass” $> 1500 \text{ GeV}$

In Table 1 we show the number of signal and background events kept and rejected by each cut (with numbers rounded to the nearest integer).

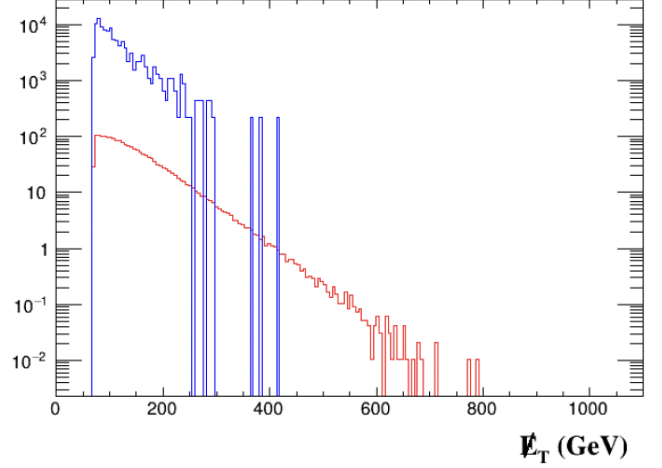


Fig. 5: Anticipated number of events for the same sets of collisions as in Fig. 4, but retaining only those events which satisfy the 9 cuts specified in Table 1. Experimentally, the “signal” events are seen as an excess over the predicted background, in the present case for 2 quark jets with missing transverse energy, after the cuts. One anticipates cuts much more sophisticated and effective than these initial attempts, of course.

cut	signal kept	signal rejected	background kept	background rejected
1	10307	13	101700400	116602100
2	9521	785	27214465	74485935
3	8848	673	19331560	7882905
4	6224	2624	2939007	16392553
5	4267	1956	869280	2069726
6	3197	1070	397747	471533
7	2236	961	160670	237076
8	2002	234	121157	39512
9	1946	56	113735	7422

Our calculated total cross-section for production of a h^0 pair accompanied by two quark jets is 20 fb at 14 TeV and 770 fb at 100 TeV. With the optimized cuts of Table 1, the cross-section for the signal (higgsos and quark jet pair) is reduced by a factor of about 5, but the background is reduced by a factor of about 2000.

More specifically, for this integrated luminosity, after the cuts there are about 1950 signal events and 114,000 background events, so that the significance, according to the simple prescription $n_s/\sqrt{n_b + n_s}$ used here and in [12] and [13], is $> 5\sigma$.

This is, in fact, our principal conclusion: If it exists, the present dark matter candidate can be detected at the high-luminosity LHC with optimized cuts.

For higher integrated luminosities, extending up to 3000 fb^{-1} , the significance reaches $> 5\sigma$ with simpler cuts – and the cuts used here are, of course, far less sophisticated (and probably less elegant) than those which can be developed

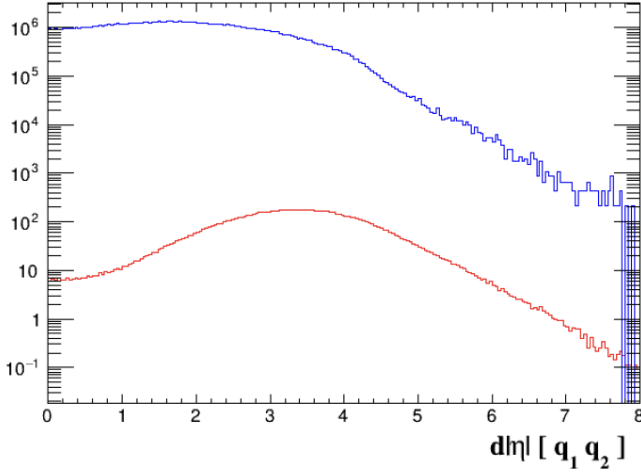


Fig. 6: Anticipated number of events for the same sets of collisions as in Fig. 4, again before cuts, as a function of $|\eta_d|$ for “vector difference” of quark momenta (in notation of [13]).

on a longer time scale, with a much more nuanced understanding of detector capabilities and limitations, as the time approaches for actual data-taking at the HL-LHC.

A calculation for the current LHC, with the same cuts but 13 TeV center-of mass-energy and and 100 fb^{-1} integrated luminosity, resulted in a significance of less than 3σ , indicating that the HL-LHC is required for credible discovery of the present particle.

The cross-sections for higgson production in Fig. 3 are an order of magnitude higher than those for VBF Higgs pair creation. We attribute this to destructive interference between the several competing processes for the Higgs that can be seen in e.g. Fig. 1 (b) of [34], plus the larger mass of the Higgs. As pointed out in [44], “All the HH production mechanisms feature the interference between diagrams that depend on the self-coupling with diagrams that do not”, and the cross-sections also decrease with increasing mass.

However, the cross-section for h^0 production at 14 TeV is only about half the total cross-section for double Higgs production at this energy when all processes are included: approximately 40 fb [44].

The calculations reported here are leading-order, but the prediction at 14 TeV should be quantitative – since the closely related LO and N³LO cross-sections for VBF Higgs pair production at this energy were found to be nearly the same [40]. At 100 TeV the results are presumably less reliable, and errors of a factor of 2 or 3 would not be surprising.

Second example – higgson pair accompanied by Z jet, with 100 TeV center of mass energy and 3000 fb^{-1} integrated luminosity. There are, of course, many other possible signals besides those in Fig. 3 (and ordinarily many Feynman diagrams corresponding to a given signal).

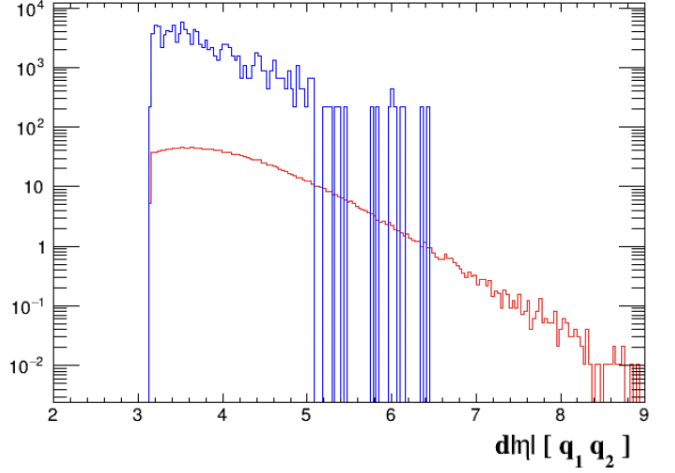


Fig. 7: Anticipated number of events for the same sets of collisions as in Fig. 4, but with the cuts of Fig. 6, as a function of $|\eta_d|$ for “vector difference” of quark momenta (in notation of [13]).

Figs. 8 and 9 show our results (again obtained with MadGraph and MadAnalysis) for one low-order independent signal: a single Z jet accompanying a higgson pair.

The cross-section is found to be a potentially achievable 6 fb before cuts. The standard model background is a Z jet accompanying a pair of neutrinos, with a cross-section of 40 pb before cuts.

The optimized cuts are:

Cut 1: “missing transverse energy” $> 500 \text{ GeV}$

Cut 2: for Z pseudorapidity $-3.5 < \eta < 3.5$

In Table 2 we show the number of signal and background events kept and rejected by each cut (with numbers again rounded to the nearest integer).

cut	signal kept	signal rejected	background kept	background rejected
1	14965	3485	70835100	49389660
2	2493	12472	169276	70665823

After the cuts of Table 2, there are about 2500 signal events and 169,000 background events, so that the significance, according to the simple prescription stated above and used in [12] and [13], is about 6σ . This then provides an independent way to detect and identify the present particle if a 100 TeV proton collider can be achieved and can acquire 3000 fb^{-1} of integrated luminosity.

Production cross-sections and experimental signatures in electron-positron and muon colliders.

– The other more powerful colliders planned for future decades include e^+e^- colliders and a $\mu^+\mu^-$ collider with center-of-mass energies up to 10 TeV. Here we will make no distinction between the lepton colliders because the results are nearly the same except at the lowest energies.

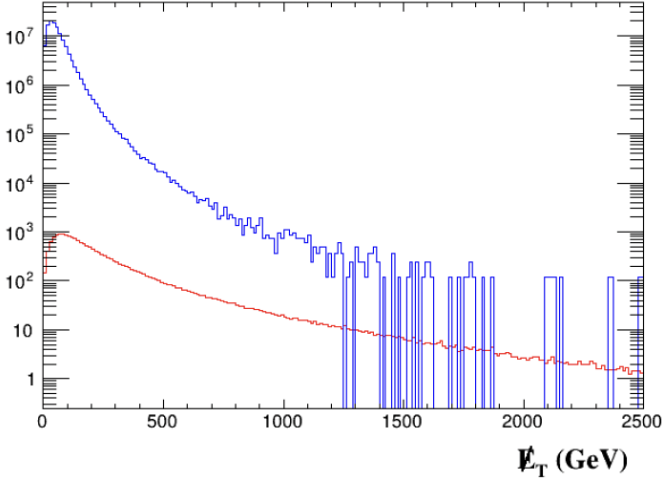


Fig. 8: Before cuts, anticipated number of events for a pair of higgses h^0 accompanied by a Z jet, as a function of “missing transverse energy” E_T . (Again, all observables are defined in [12] and [13].) The neutrino background is orders of magnitude larger than the signal, but more concentrated toward lower energy, making this a natural choice for the first cut. (The relatively large size of the fluctuations in the background histograms is explained in the caption to Fig. 4.)

Two simple processes are shown in Fig. 10: vector boson fusion (VBF) and Z-strahlung. In our calculations, simple VBF with W bosons has a sizable cross-section at high energy – about 700 fb at 10 TeV for polarized muon beams – but this process is unobservable because only higgses and neutrinos are produced.

Our results for the simplest observable processes are shown in Fig. 11. The cross-sections are unfortunately small – below 0.3 fb even for polarized beams at the highest energies. This means that detection of the present particle at lepton colliders will be challenging.

Cross-section for direct detection . – The lowest-order coherent processes for scattering of the present particle off a nucleus are represented by Fig. 4 of [1]. For a dark matter particle with initial velocity $v \ll c$ it is a good approximation to neglect both initial and final velocities. It is also a good approximation to neglect all but the valence u and d quarks. (In the familiar scattering through Higgs exchange [46, 47], all 6 quarks make comparable contributions, because the heavy quarks have stronger couplings. But here all quarks have comparable couplings, and the number density is relatively low even for strange quarks.)

The interior loop for each amplitude, involving a given virtual quark with mass $m(p)$ (within a nucleon, at energy scale p) and a given vector boson (or its Goldstone boson)

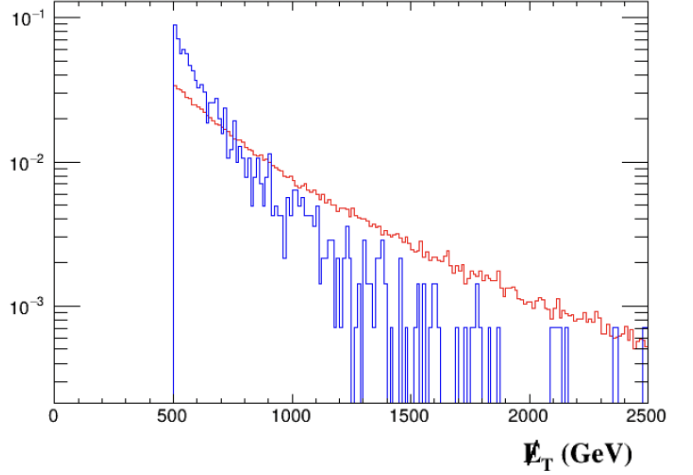


Fig. 9: After the cuts specified in Table 2, anticipated number of events for higgses pair accompanied by Z jet, as a function of E_T – scaled to one in this plot to emphasize the difference in E_T for signal and background.

with mass M , involves

$$\int \frac{d^4 p}{(2\pi)^4} \frac{-1}{(p^\mu p_\mu - M^2 + i\epsilon)^2} \frac{i(\not{p} + m(p))}{p^\mu p_\mu - m(p)^2 + i\epsilon} \approx -i \int \frac{d^4 p}{(2\pi)^4} \frac{1}{(p^\mu p_\mu - M^2 + i\epsilon)^2} \frac{m(p)}{p^\mu p_\mu + i\epsilon} \quad (1)$$

since the integral over \not{p} is odd in p_μ and $m(p) \ll M$. Here $m(p)$ is the effective quark mass at momentum p . In the original right-hand factor the 4-momentum is $p' = p + p_0$, where p_0 is the momentum of the incident quark. But we can rename the momentum, with $p' \rightarrow p$ and $p \rightarrow p - p_0$ in the volume element and other factor. Then neglecting p_0 in this other factor introduces only a small error in the integral, and we obtain the form on the left side of (1).

This loop integral is manifestly convergent and it can be evaluated as a simple integral over the Euclidean momentum after a Wick rotation – or alternatively using the residue theorem for p_0 , followed by 3-dimensional integration. The result is

$$I = \frac{1}{16\pi^2} \frac{m(M)}{M^2}. \quad (2)$$

For each amplitude this integral is multiplied by a set of factors – involving the metric tensor $g_{\mu\nu}$ (in the W or Z propagator), gamma matrices γ^μ and gauge generators (at vertices), and couplings proportional to the weak interaction coupling constant g – which turns out to reduce in each case to a simple overall factor λ proportional to g^4 that is $\sim 0.02 - 0.1$, depending on the diagram. (W^+W^- and W^-W^+ diagrams must be combined.)

The effective interaction with a given initial quark q in a nucleon N is then $\lambda I \langle N | \bar{q} q | N \rangle$, where $\langle N | \bar{q} q | N \rangle$ is the expectation value of the number of these quarks in the

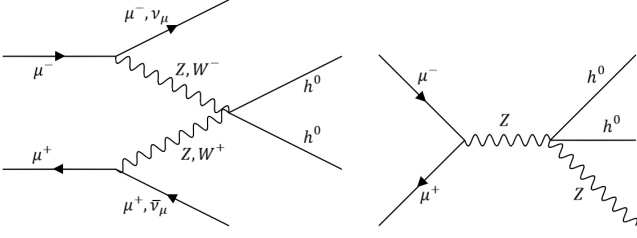


Fig. 10: Production via vector boson fusion and Z-strahlung.

nucleon. Notice that, in I , $m(p)$ is the mass of the central virtual quark – e.g., a u if the initial and final quarks are d and the vector bosons are W^\pm .

For Higgs exchange in the case of a hypothetical scalar particle having a Higgs-boson coupling $\lambda_\chi v$, where v is the Higgs-field vacuum expectation value, the effective interaction with a given quark, having effective mass m_q and effective Yukawa coupling $y_q = m_q/v$, is $\langle N|\bar{q}q y_q|N\rangle_{eff} \lambda_\chi v/M_H^2 = \lambda_\chi \langle N|\bar{q}q m_q|N\rangle_{eff}/M_H^2$, where M_H is the Higgs mass.

Then the difference between the present loop process and Higgs exchange is that the amplitude is reduced by a factor of

$$\frac{6 (16\pi^2)^{-1} [\lambda \langle N|\bar{q}q|N\rangle m(M)/M^2]_{val,avg}}{6 \lambda_\chi [\langle N|\bar{q}q m_q|N\rangle]_{eff,avg}/M_H^2} = \frac{1}{16\pi^2} \frac{M_H^2}{M_{avg}^2} \frac{[\lambda \langle N|\bar{q}q|N\rangle m(M)]_{val,avg}}{\lambda_\chi [\langle N|\bar{q}q m_q|N\rangle]_{eff,avg}} \quad (3)$$

where $[\dots]_{val,avg}$ is an average over the valence quarks within a nucleon N and their interactions with W and Z bosons, $[\dots]_{eff,avg}$ is the average of the effective value of the product over all 6 quarks, the averages are also over both nucleon species, and M_{avg} is an average over W and Z masses.

Since $(M_H^2/M_{avg}^2) \lambda \sim 0.1$, if we had $[\langle N|\bar{q}q|N\rangle m(M)]_{val,avg} \approx [\langle N|\bar{q}q m_q|N\rangle]_{eff,avg}$, the amplitude for the present process would be lowered only by about $0.1 (16\pi^2)^{-1} / \lambda_\chi \sim 10^{-3} / \lambda_\chi$. But the appropriate value of $\langle N|\bar{q}q|N\rangle$ for a valence quark is roughly $1/6$, and the appropriate values of $m(p)$ at high energy are the current (“free quark”) masses, which are about 2.4 MeV and 4.8 MeV for up and down quarks respectively, so that $[\langle N|\bar{q}q|N\rangle m(M)]_{val,avg} \sim 0.0005$ GeV, whereas $[\langle N|\bar{q}q m_q|N\rangle]_{eff,avg} \sim 0.05$ GeV [46, 47]. The amplitude for the present loop process is then reduced, relative to that for Higgs exchange, by a further factor of $\sim 10^{-2}$, or by $\sim 10^{-5} / \lambda_\chi$ overall, implying that the cross-section is lowered by $\sim 10^{-10} / \lambda_\chi^2$. Since $\lambda_\chi = 0.01/4$ for a particle of mass 100 GeV would imply a Higgs-exchange cross-section of $\sim 10^{-46}$ cm² [47], for the present process this will be lowered to $\sim 10^{-51}$ cm².

The cross-section for direct detection of the present dark matter candidate is then $\sim 10^{-51}$ cm², which is below

the sensitivities of current and planned detectors and well within the neutrino fog. This estimate is confirmed by detailed calculation within a parton description, but an accurate result would require sophisticated treatment of form factors, parton distribution functions, higher-order processes, and other issues involving interactions for a loop process inside a nucleus.

If $m(p)$ in (1) and (2) were taken to be the mass of a constituent quark, the predicted cross-section would be above 10^{-48} cm² and within range of current experiments [48–50]. But the appropriate mass at high energy (and a short time scale) is instead the current mass, which is much smaller, reducing the cross-section by orders of magnitude.

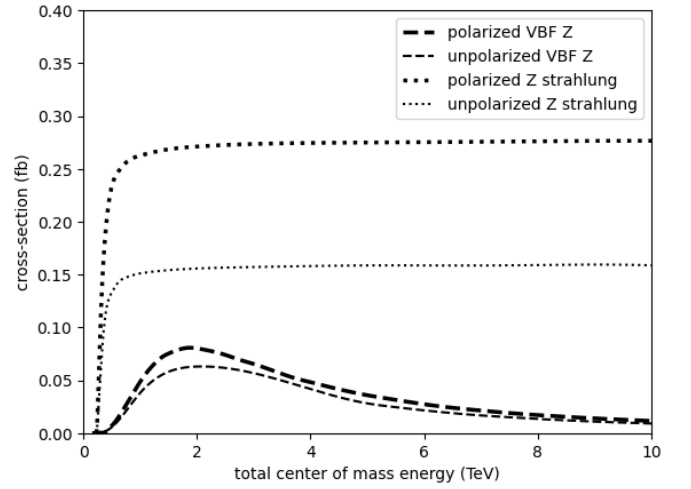


Fig. 11: Cross-sections for the processes of Fig. 10.

Conclusions. — Based on the calculations above, we conclude that the present dark matter WIMP is consistent with all current experimental and observational constraints, and (1) its mass is about 70 GeV if it is the dominant dark matter particle (although somewhat larger in a multicomponent scenario); (2) the annihilation cross-section and mass are consistent with those inferred from gamma-ray and antiproton observations based on a dark matter interpretation; (3) it should be detectable in the high-luminosity LHC with $> 5\sigma$ statistical significance; (4) it should be observable with additional signatures in more powerful future proton colliders; (5) separating signal from background will be challenging in an e^+e^- or muon collider; (6) direct detection will also be challenging, since the cross-section is $\sim 10^{-51}$ cm².

Our principal conclusion is that this particle should be detectable at the high-luminosity LHC, perhaps after only two years with an integrated luminosity of 500 fb⁻¹.

It can also be observed and identified in further astrophysical observations, in the experiments planned for future colliders, and possibly through direct detection with extended capabilities such as directional detection.

REFERENCES

- [1] Reagan Thornberry et al., EPL [Europhysics Letters] 134, 49001 (2021), arXiv:2104.11715 [hep-ph].
- [2] Caden LaFontaine et al., Universe 7, 270 (2021), arXiv:2107.14390 [hep-ph].
- [3] Bailey Tallman et al., Letters in High Energy Physics LHEP-342 (2023), arXiv:2210.15019 [hep-ph].
- [4] Bailey Tallman et al., proceedings of the 41st International Conference on High Energy Physics, ICHEP 2022, arXiv:2210.05380 [hep-ph].
- [5] “Dark Matter”, Section 27 of S. Navas et al. (Particle Data Group), Phys. Rev. D 110, 030001 (2024), https://pdg.lbl.gov/2024/reviews/contents_sports.html, and references therein.
- [6] Rebecca K. Leane et al. (Topical Group on the Cosmic Frontier for Snowmass 2021), arXiv:2203.06859 [hep-ph].
- [7] Jodi Cooley et al. (Topical Group on Particle Dark Matter for Snowmass 2021), arXiv:2209.07426 [hep-ph].
- [8] Antonio Boveia et al. (Topical Group on Dark Matter Complementarity for Snowmass 2021), arXiv:2211.07027 [hep-ex].
- [9] 2023 Particle Physics Project Prioritization Panel, <https://arxiv.org/pdf/2407.19176>.
- [10] Marco Cirelli, Alessandro Strumia, and Jure Zupan, arXiv:2406.01705 [hep-ph].
- [11] G. Bélanger, F. Boudjema, and A. Pukhov, arXiv:1402.0787 [hep-ph]; G. Alguero, G. Bélanger, F. Boudjema, et al., arXiv:2312.14894 [hep-ph]; <https://lapth.cnrs.fr/micromegas/>.
- [12] J. Alwall et al., JHEP 07, 079 (2014), arXiv:1405.0301 [hep-ph]; <http://madgraph.phys.ucl.ac.be/>.
- [13] Eric Conte, Benjamin Fuks, and Guillaume Serret, Comput. Phys. Commun. 184, 222 (2013), arXiv:1206.1599 [hep-ph]; <https://github.com/MadAnalysis/madanalysis5>, <https://madanalysis.irmp.ucl.ac.be/>.
- [14] Eleonora Di Valentino et al., Class. Quantum Grav. 38, 153001 (2021), arXiv:2103.01183 [astro-ph.CO], and references therein.
- [15] M. L. Ahnen et al. (MAGIC Collaboration), JCAP 02, 039 (2016), arXiv:1601.06590 [astro-ph.HE].
- [16] Alexandre Alvarez et al., JCAP 09, 004 (2020), arXiv:2002.01229 [astro-ph.HE].
- [17] A. Acharya et al. (VERITAS Collaboration), arXiv:2407.16518 [astro-ph.HE].
- [18] Lisa Goodenough and Dan Hooper, arXiv:0910.2998 [hep-ph].
- [19] Vincenzo Vitale and Aldo Morselli (for the Fermi/LAT Collaboration), arXiv:0912.3828 [astro-ph.HE].
- [20] Lisa Goodenough and Dan Hooper, Phys. Lett. B 697, 412 (2011), arXiv:1010.2752 [hep-ph].
- [21] Christopher Karwin et al., Phys. Rev. D 95, 103005 (2017), arXiv:1612.05687 [hep-ph], and references therein.
- [22] Rebecca K. Leane et al., Phys. Rev. D 98, 023016 (2018), arXiv:1805.10305 [hep-ph].
- [23] Rebecca K. Leane and Tracy R. Slatyer, Phys. Rev. Lett. 123, 241101 (2019), arXiv:1904.08430 [astro-ph.HE], and references therein.
- [24] Alessandro Cuoco, Michael Krämer, and Michael Korsmeier, Phys. Rev. Lett. 118, 191102 (2017), arXiv:1610.03071 [astro-ph.HE].
- [25] Ming-Yang Cui et al., Phys. Rev. Lett. 118, 191101 (2017), arXiv:1610.03840 [astro-ph.HE].
- [26] Alessandro Cuoco et al., JCAP 10, 053 (2017), arXiv:1704.08258 [astro-ph.HE].
- [27] Alessandro Cuoco et al., Phys. Rev. D 99, 103014 (2019), arXiv:1903.01472 [astro-ph.HE].
- [28] Ilias Cholis, Tim Linden, and Dan Hooper, Phys. Rev. D 99, 103026 (2019), arXiv:1903.02549 [astro-ph.HE].
- [29] Minjin Jeong (on behalf of the IceCube Collaboration), arXiv:2407.16371 [astro-ph.HE].
- [30] Planck Collaboration, arXiv:1807.06209 [astro-ph.CO]. See Fig. 46.
- [31] Dan Hooper et al., Phys. Rev. D 96, 103013 (2017), arXiv:1702.08436 [astro-ph.HE].
- [32] Katherine Freese et al., Rep. Prog. Phys. 79, 066902 (2016), arXiv:1501.02394 [astro-ph.CO], and references therein.
- [33] FCC Collaboration, Eur. Phys. J. Special Topics 228, 755 (2019), <https://www.usparticlephysics.org/2023-p5-report/>.
- [34] J. Baglio et al., JHEP, 04, 151 (2013), arXiv:1212.5581 [hep-ph].
- [35] R. Frederix et al., Phys. Lett. B 732, 142 (2014), arXiv:1401.7340 [hep-ph].
- [36] Liu-Sheng Ling et al., Phys. Rev., D 89, 073001 (2014), arXiv:1401.7754 [hep-ph].
- [37] Matthew J. Dolan et al., Eur. Phys. J. C 75, 387 (2015), arXiv:1506.08008 [hep-ph].
- [38] D. de Florian et al., arXiv:1610.07922 [hep-ph].
- [39] Fady Bishara, Roberto Contino, and Juan Rojo, Eur. Phys. J. C 77, 481 (2017), arXiv:1611.03860 [hep-ph].
- [40] Frédéric A. Dreyer and Alexander Karlberg, Phys. Rev. D 98, 114016 (2018), arXiv:1811.07906 [hep-ph].
- [41] Ernesto Arganda, Claudia Garcia-Garcia, and Maria Jose Herrero, Nuclear Physics B 945 (2019), arXiv:1807.09736 [hep-ph].
- [42] M. Cepeda et al., arXiv:1902.00134 [hep-ph].
- [43] B. Di Micco et al., Reviews in Physics 5, 100045 (2020), arXiv:1910.00012 [hep-ph].
- [44] Michelangelo L. Mangano, Giacomo Ortona, and Michele Selvagg, Eur. Phys. J. C 80, 1030 (2020), arXiv:2004.03505 [hep-ph].
- [45] M. Carena et al., in R.L. Workman et al. (Particle Data Group), Prog. Theor. Exp. Phys. 2022, 083C01 (2022) and 2023 update, <https://pdg.lbl.gov/index.html>.
- [46] John Ellis, Natsumi Nagata, and Keith A. Olive, Eur. Phys. J. C 78, 569 (2018), arXiv:1805.09795 [hep-ph].
- [47] Yann Mambrini, *Particles in the Dark Universe* (Springer, 2021).
- [48] E. Aprile et al. (XENON), arXiv:2502.18005 [hep-ex].
- [49] J. Aalbers et al. (LZ), Phys. Rev. Lett. 131, 041002 (2023), arXiv:2207.03764 [hep-ex].
- [50] Z. Bo et al. (PandaX), Phys. Rev. Lett. 134, 011805 (2025), arXiv:2408.00664 [hep-ex].